Materials Chemistry and Physics 205 (2018) 470–479

Contents lists available at ScienceDirect

Materials Chemistry and Physics

journal homepage: www.elsevier.com/locate/matchemphys

The effect of initial moisture content of cation-exchange resin on the preparation and properties of heterogeneous cation-exchange membranes

Pavel Bulejko [a, b], Eliška Stránská [b, *]

[a] Heat Transfer and Fluid Flow Laboratory, Faculty of Mechanical Engineering, Brno University of Technology, Technická 2, 616 69 Brno, Czech Republic
[b] Membrain s.r.o, Pod Vinicí 87, 471 27 Stráž pod Ralskem, Czech Republic

HIGHLIGHTS

- CEMs were prepared of resin varying in moisture content.
- The moisture's effect on resin grinding and CEM blending/extrusion are discussed.
- The influence of moisture on electrochemical and mechanical properties is studied.
- CEM resistance increases when increasing initial resin moisture content.
- IEC decreases while permselectivity varies with resin moisture content.

GRAPHICAL ABSTRACT

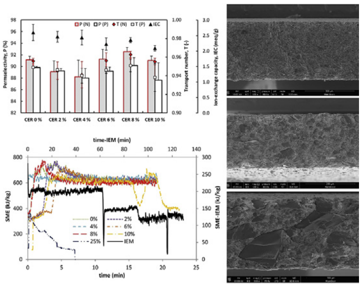

ARTICLE INFO

Article history:
Received 11 September 2017
Received in revised form
9 November 2017
Accepted 24 November 2017
Available online 27 November 2017

Keywords:
Moisture
Ion-exchange resin
Ion-exchange membrane
Electrochemical properties
Mechanical properties

ABSTRACT

This work deals with the influence of moisture content of cation-exchange resin (CER) on the properties of prepared cation-exchange membranes (CEMs). CER was dried and moistened to 2, 4, 6, 8, 10 and 25% and then milled using a vibratory mill. The CER was then mixed with low density polyethylene and extruded to prepare CEMs. Some of the samples were further hot-pressed. The CEMs were then characterized in terms of their mechanical and electrochemical properties, including specific and areal resistance, ion-exchange capacity (IEC), permselectivity and transport number. The results showed that resistance increases with increasing moisture content. IEC decreases with increasing moisture while permselectivity strongly varies with moisture content.

1. Introduction

Ion-exchange membranes (IEMs) are essential in electro-separation processes such as electrodialysis (ED) [1–3], electro-deionization [2,4,5], membrane electrolysis [6,7], and in power storage and generation (fuel cells and redox flow batteries) [8–10]. Recently, reverse ED has also become of greater interest [11–15]. IEMs are basically divided into, either cation and anion exchange membranes according to the ions they transfer/retain, or homogeneous and heterogeneous according to the IEM's composition [3]. Homogeneous IEMs are mostly comprised of a foil made of pure

---

[*] Corresponding author. Membrain s.r.o, Pod Vinicí 87, 471 27 Stráž pod Ralskem, Czech Republic.

E-mail address: Eliska.Stranska@membrain.cz (E. Stránská).

https://doi.org/10.1016/j.matchemphys.2017.11.049
0254-0584/

ion-exchange resin (IER) material, and therefore have supreme electrochemical properties but mostly poor mechanical properties. Conversely, a heterogeneous IEM is a functional composite made of a finely milled IER, a polymeric binder and a reinforcing fabric [1,3,16]. Together, these components ensure the required electrochemical properties (though lower than homogeneous IEMs) and also necessary mechanical properties for the aforementioned processes. The IER has the most influence on electrochemical/transport properties of an IEM, i.e. ion-exchange capacity (IEC), electrical conductivity and permselectivity. Moreover, these properties determine the other characteristics of the electro separation process, including separation efficiency and energy consumption, hence the cost of the overall process and applicability for larger industrial scales.

Many IERs are based on a copolymer of styrene and divinylbenzene, with bonded ion-exchange groups usually in the form of spherical beads or ground particles, which ensure the exchange of a selected ionic species [17]. To ensure an adequate surface area and blending with the polymer matrix without detrimental structural defects, IER is most often ground to particle sizes ranging from 1 to 50 μm [18]. Therefore, the particle-size distribution of IER is very important. The particle-size distribution is mainly influenced by the type of milling equipment, milling time and properties of the material to be milled (IER), the latter of which is related to the material moisture content. A higher IER moisture content or direct contact with water not only causes IER particles to swell, but also reduces their grindability, bulk properties and thus the complete preparation of IEMs. Moreover, moisture content affects the transport properties of the IEMs [19–21] and influences the morphology of ion-exchange polymers [22].

In practice, many manufacturers supply IERs in a fully swollen state, containing about 45–60% of water depending on type. This water must be removed before use for IEM preparation, which is done using a fluidized bed dryer to a theoretical value of 0%, even though there is always some moisture remaining. The IER moisture must be lower than 4% to be used in IEM production. Several studies have analysed the influence of IEM water content/transport either on a purely theoretical [23–25] or practical level by considering the IEM structure itself [26–28] or IEM-involved processes such as electrodialysis [29–31]. These works studied the influence of the overall water uptake of prepared IEMs and/or the influence of different humidity levels on transport properties. However, the influence of initial moisture of an IER on IEM preparation itself and its properties has not yet been studied. Therefore, this work aimed to determine the influence of IER (cation-exchange resin – CER) moisture on milling, CER/polymer matrix blending, extrusion and IEM hot pressing in relation to their final transport and mechanical properties. Transport properties were evaluated in terms of electrical resistance, IEC and permselectivity (transport number). These parameters were further compared between IEMs prepared by extrusion with subsequent hot pressing as well as non-pressed IEMs.

2. Experimental

2.1. Preparation of IER varying in moisture content

CER from Suqing (Jiangsu Suqing Water Treatment Engineering Group Co. Ltd., China) in bead form was used (Table 1). It has an optimal ion-exchange capacity/swelling capacity ratio. The CER is based on cross-linked polystyrene-co-divinylbenzene (PS-DVB) with sulfonic (CER) ion-exchange groups and is often used for production of heterogeneous IEMs. The CER was first washed and then dried at 130 °C using a fluidized-bed dryer to a minimum moisture content of about 0.5%. This value was considered referential, i.e. 0% of moisture. The CER was modified to 2%, 4%, 6%, 8%, 10% and 25% moisture content as follows. Water content φ of the IER was calculated as follows:

Table 1
Properties of CER used.

Type	Suqing 001x7Na, gel, strong acid
IEC[a] (meq g^{-1})	4.50
IEC[b] (meq g^{-1})	5.33
Swelling capacity[b] (cm^3 g^{-1})	2.52
Water content[a] (%)	45–50
Water content[b] (%)	49.9

[a] Product data sheet [32].
[b] Measured.

$$\varphi = \frac{m_w - m_d}{m_d} 100 \tag{1}$$

where m_w and m_d are weights of wet and dry IER, respectively. The modified CER was milled using a Vibrom 42S vibrational mill filled with steel cylinders with dimensions of 12 × 12 mm and a weight of 170 kg. The CER was milled for 15 min at a vibrations frequency of 50 Hz and discharged for 20 + 2 min at 35 + 25 Hz. The particle-size distribution of the milled resin was measured using a Malvern Mastersizer 2000 laser diffraction analyzer.

2.2. Membrane preparation

The milled CER samples with varying moisture content were blended with low density polyethylene (LDPE) in a mixer at 140 °C to prepare pellets. The amount of CER was 62% per weight of LDPE. The pellets were extruded to prepare membranes. Some membranes were further hot-pressed at 135 °C for 5 min at 25 bars and cooled down to 60 °C to compare against the properties of non-pressed membranes. Both homogenization and extrusion were performed in a HAAKE PolyLab OS Rheo Drive 16 machine (ThermoScientific). A PTW 24/28 twin screw (diameter and length/diameter ratio were 24 and 28, respectively) was used for homogenization and a Rheomex 19/25 single screw for extrusion, both with a compression ratio of 2:1. The materials to be blended were dosed to the mixer using Congrav® OP1T CB Plus feeders (Brabender Technologie GmbH & Co. KG) with a twin screw and a single screw for CER and LDPE, respectively, with a frequency of 60 rpm. The parameters of extrusion were recorded in software, including the revolution speed, torque, pressure on the extrusion head, and pressure in front of the extrusion head. The extruder response was expressed using the specific mechanical energy calculated as follows [33–35]:

$$SME(\text{kJ/kg}) = \frac{2\pi \cdot n \cdot T}{MFR} \tag{2}$$

where n is the screw revolution speed (min^{-1}), T is the screw (motor) torque (N·m) and MFR is the mass flow rate (g/min) given by the dosing speed of CER and LDPE, which is 43.86 g/min. SME reflects the work input from the motor into the material during the blending/extrusion i.e. the shearing energy exerted to the composite [35].

2.3. Membrane characterization

2.3.1. Ion-exchange capacity (IEC)

IEC is the number of equivalents of bound dissociated groups in IEM related to the weight of dry matter [36]. The method to determine IEC is described elsewhere [37]. Briefly, the sample (granules) was immersed in demi water for 8 h, then conditioned in 1 M NaOH and 1 M HCl for 8 and 12 h, respectively. Lastly, the samples soaked in demi water for 2 h and dried at a temperature of 105 °C. The dried CER sample was then soaked in 50 ml (V_{NaOH}) of 0.1 M NaOH solution (c_{NaOH}) for 1 h, and 10 ml of this solution (V^{I}_{NaOH}) was then titrated by 0.1 M HCl (c_{HCl}) using a Metrohm 682 titroprocessor with a combined glass electrode. The IEC was then calculated as follows:

$$IEC = \frac{\left(c_{NaOH} - \frac{c_{HCl}V_{HCl}}{V^{I}_{NaOH}}\right)V_{NaOH}}{m_{CER}} \tag{3}$$

where V_{HCl} is the volume of titrated HCl and m_{CER} is the weight of the dried sample.

2.3.2. Specific and areal electric resistance

The measurement of electrochemical resistances was carried out using the compensatory method [37], using a measuring cell as described in Refs. [1,29,38] at a constant direct current of 10 mA and a temperature of 25 °C. The cell consists of two conical compartments separated by membrane specimen. Each compartment contain platinum electrodes (providing constant direct current controlled by an ammeter), reference calomel electrodes and temperature sensors (to control the temperature of the solution). Each compartment was filled with 0.5 M NaCl solution and the potential gradient in the membrane/solution system was scanned using reference calomel electrodes. The same was then measured in the system without the membrane sample at the same constant conditions. The electric resistances were then calculated using the following equations [2,38]:

$$R^{s}_{j} = \frac{\left|U^{s}_{meas}(1,2) - U^{r}_{as}(1,2)\right|_{j} + \left|U^{s}_{meas}(2,1) - U^{r}_{as}(2,1)\right|_{j}}{2I} \tag{4}$$

$$R^{s+m}_{j} = \frac{\left|U^{s+m}_{meas}(1,2) - U^{s+m}_{as}(1,2)\right|_{j} + \left|U^{s+m}_{meas}(2,1) - U^{s+m}_{as}(2,1)\right|_{j}}{2\ I} \tag{5}$$

$$R_{A,j} = \left(R^{s+m}_{j} - \overline{R}^{s}\right)A_{m} \tag{6}$$

$$R_{S,j} = \left(R^{s+m}_{j} - \overline{R}^{s}\right)\frac{A_{m}}{th_{j}} \tag{7}$$

where $R^{\mathrm{s}}_{\mathrm{j}}$ is the resistance without the membrane, $R^{\mathrm{s+m}}_{\mathrm{j}}$ is the resistance with the membrane (indices s and m are solution and membrane, respectively, and j is the solution type), $R_{\mathrm{A,j}}$ is the membrane areal resistance, $R_{\mathrm{S,j}}$ is the specific resistance, U_{meas} is the measured potential under the current, U_{as} is the asymmetric potential measured without applied current, A_{m} is the active membrane sample area (0.7655 cm^2), th_{j} is the sample thickness, (1,2) and (2,1) denote the sequence of the saturated calomel electrode.

2.3.3. Permselectivity and transport number

Permselectivity describes the ability of IEM to prevent co-ions from passing through [15] and is often discussed with transport number [39]. The transport number of ions is a quantitative and complex characteristic of the membrane selectivity and represents the fraction of current transferred by certain ions. This parameter strongly depends on experimental conditions [19]. It was determined according to the Henderson method [1,37]. Samples were equilibrated in a 0.5 M KCl solution for 24 h prior to measurement. The principle consists in measuring the membrane potential between two solutions with different concentrations (0.1 and 0.5 M KCl) separated by the membrane sample without current load. The resulting potential between reference silver chloride electrodes due to the concentration gradient was measured. There is a relationship between membrane potential ΔE_{M} and cation transport number t_{C} (permselectivity Pm_{C}):

$$\Delta E_{M} = -\frac{RT}{2F}(2t_{C} - 1)\ln\frac{a_{C,1}a_{A,1}}{a_{C,2}a_{A,2}} = -\frac{RT}{2F}Pm_{C}\ln\frac{a_{C,1}a_{A,1}}{a_{C,2}a_{A,2}} \tag{8}$$

where a_{C1}, a_{C2} and a_{A1}, a_{A2} are activities of cations and anions in solutions 1 and 2, respectively, and T, R, and F are temperature, the molar gas constant, and Faraday's constant, respectively. The relationship between transport number of cation t_{C} and anion $t_{\mathrm{A,}}$ is as follows:

$$t_{C} + t_{A} = 1 \tag{9}$$

2.3.4. Membrane structure and mechanical properties

The morphology of the prepared membranes (membrane cross-section) was investigated using a Quanta 250 FEG scanning electron microscope. The IEM samples were broken in liquid nitrogen and a layer of chrome was then sputtered on the cross-section surface using a Q150T S/E/ES Quorum Technologies sputter. SEM images were then taken at a source voltage of 10 kV and a chamber pressure of 80 Pa. A large field detector for secondary electrons was used. The distance from sample was 10 mm.

The mechanical properties, i.e. Young's modulus of elasticity, strength and elongation were determined from stress strain curves

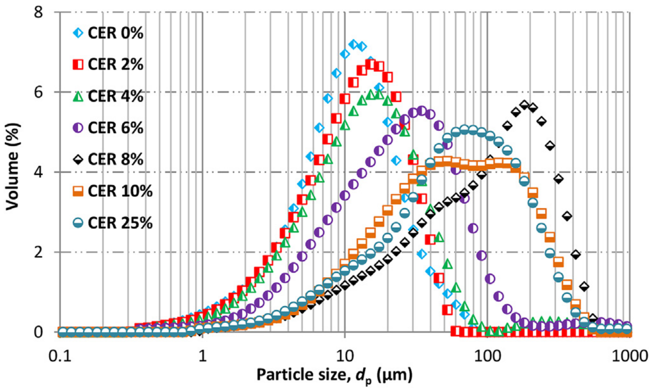

Fig. 1. Particle-size distributions of CER with varying moisture content.

measured in accordance with CSN EN ISO 527-3 [40] using a Tinius Olsen H5KT tensile testing machine with a speed of 15 mm min^{-1} and a clamping length of 50 mm.

3. Results and discussion

3.1. Effect of moisture content on CER grinding

Fig. 1 shows the particle size distribution of milled CER varying in moisture content. As expected, with increasing moisture the particle size increases up to 8% of moisture. CER with 8% moisture content has its particle size modus above 100 μm. The same is true for CER with 10 and 25% moisture content. These cannot be processed further for membrane preparation (described later). CER 25% formed a paste-like material and it was not possible to discharge this material from the mill. The material was flushed out of the mill with water.

CER 10% was also very complicated to process due to its sticking to grinding bodies, although part of the CER was usable and several samples were prepared. Moreover, there were other problems related to corrosion of grinding bodies caused by the water flushing. For the samples with 8% moisture content or less, the particle size distribution curves are shifted to higher sizes due to the swelling of the CER particles and increased adhesion forces causing formation of agglomerates which are poorly dispersible. Moreover, swollen CER is less brittle (has a higher toughness) so grinding is less efficient and its intensity is not very high over the constant grinding time.

3.2. Changes of blending/extrusion parameters with varying CER moisture

In this section, the processing parameters of membrane preparation are discussed. Principally, there are two important parameters to control the mixing performance of the extruder: screw speed and residence time, i.e. the time between delivery of the material to the extruder hopper and the first extrudate leaving the extrusion head [41]. Varying the screw speed can provide the required mechanical shear rate and shear stress for better dispersion of IER particles throughout the LDPE matrix. Additionally, by varying the speed of feeders, residence time can be controlled to achieve appropriate blending. This also depends on the difficulty of aggregate breakup, which is more complicated with higher moisture. To compare the extruder response in relation to material properties with varying IER moisture, the screw speed was kept constant. Thus the torque and pressures are clearly given by changes of the material properties due to changes in moisture of IER and its rheological behaviour during processing.

Fig. 2 shows the specific mechanical energy (SME) and extrusion head pressures during blending and subsequent extrusion of the IER/matrix mixture pellets and membrane foils. All curves are characteristic of a typical start, up to 5 min. At this point, the homogenizer is fed with LDPE, then CER is added in the required percentage, causing the screw torque and extrusion head pressure to gradually increase, thus increasing SME. Generally, lower torque (about 100 Nm) is often appropriate. If torque exceeds 150 Nm the process will stop due to a shear pin rupture. The pressure on the extrusion head should not be higher than 100 bars or the device will automatically shut down.

The SME reached a maximum value of about 800 kJ/kg (up to 5 min of blending), then slightly decreased to an equilibrium course of about 600 kJ/kg (up to 10 min) and then mostly stayed constant. The decrease can be caused by slight polymer degradation or by the thixotropic effect accompanied by a temporary reduction of blend viscosity. This decrease is useful and helps to easily process the polymer blend and increase the extruder throughput, keeping the torque within the limits [35]. There were, however, several exceptions from this course, mainly for samples with higher moisture i.e. the 10% and 25% samples.

It was not possible to fully process the CER 25% sample (Fig. 2) due to its high moisture content, which caused bad rheological behaviour and high water evaporation from the material when the process temperature was at 140 °C. Therefore, the processing of this sample was stopped after 7 min and not taken for evaluation of electrochemical or mechanical properties. CER 10% proceeded normally until 15 min of processing, when a small decline was obvious. This decline was probably caused by local inhomogeneities of the material due to agglomerated resin. The moist CER could not be accurately dosed, causing torque/SME and pressure to locally fluctuate. Dosing is the main problem during blending of moist CER with LDPE. Moist CER forms clumps and the feeders, which are controlled by weight decrease on scales, are not able to dose the CER equally. Therefore, if a larger CER clump is introduced into the homogenizer, the feeders measure a higher weight decrease on the scales and slow the screw down. This causes the CER amount to locally decrease in the homogenizer, so the resulting pellets are less filled with CER. Conversely, if a large CER clump is then introduced to the homogenizer the final pellets will be overfilled. Also after homogenizer shutdown caused by locally higher pressure and torque values, the extrusion head must be dismantled and the blocking material removed to make the screw move. This was most evident with CER 25%, where the final pellets were very inhomogeneous and foam-like due to moisture release in the form of steam.

3.3. Impact of moisture content on electrochemical properties

3.3.1. IEC and permselectivity (transport number)

Fig. 3a shows IEC (measured on pellets). IEC decreased with increasing moisture content from 2.595 to 2.086. Fig. 3b and c show permselectivity and transport number of pressed (P) and non-pressed (N) membranes. Permselectivity (Fig. 3b) varies randomly for both (P) and (N) membranes. For (N), it decreases up to 4% moisture from 0.91 to 0.88 then an increase occurs up to 8% to 0.93 and then decreases again to 0.91. Permselectivity of (P) membranes follows a similar trend and is lower than that of (N) for all samples except CER 2%. The transport number (Fig. 3c) follows the same trends as permselectivity and ranges between 0.941 and 0.963 for (N) and 0.938 and 0.951 for (P).

IEC is mainly influenced by the particle size distribution of IER which is related to concentration of functional groups. The lower the particle size the higher the active surface area and thus the number of functional groups which can actively participate in ion transport. This is also related to the formation of a conductive channel through the membrane, made easier if the CER is finer and uniformly distributed throughout the membrane. Therefore, IEC decreases with higher CER moisture content. Moreover, the CER is dosed based on its weight, in other words, together with moisture. The moisture is evaporated during the homogenization, resulting in the lower weight of dry CER and causing lower IEC.

From the permselectivity definition it follows that its decrease must be caused by co-ion transfer. The Donnan theory assumes co-ion sorption decreases with increasing fixed charge concentration. As sorption of co-ions is related to their transport, a lower fixed charge concentration in the membrane is supposed to reduce permselectivity [42]. With the influence of swelling, there is a greater number of channels for co-ions formed along IER particles [1]. This means that IEMs absorbing more water (higher water uptake) tend to have lower selectivity. This may also be the reason for permselectivity decreasing up to 4% moisture. However, by

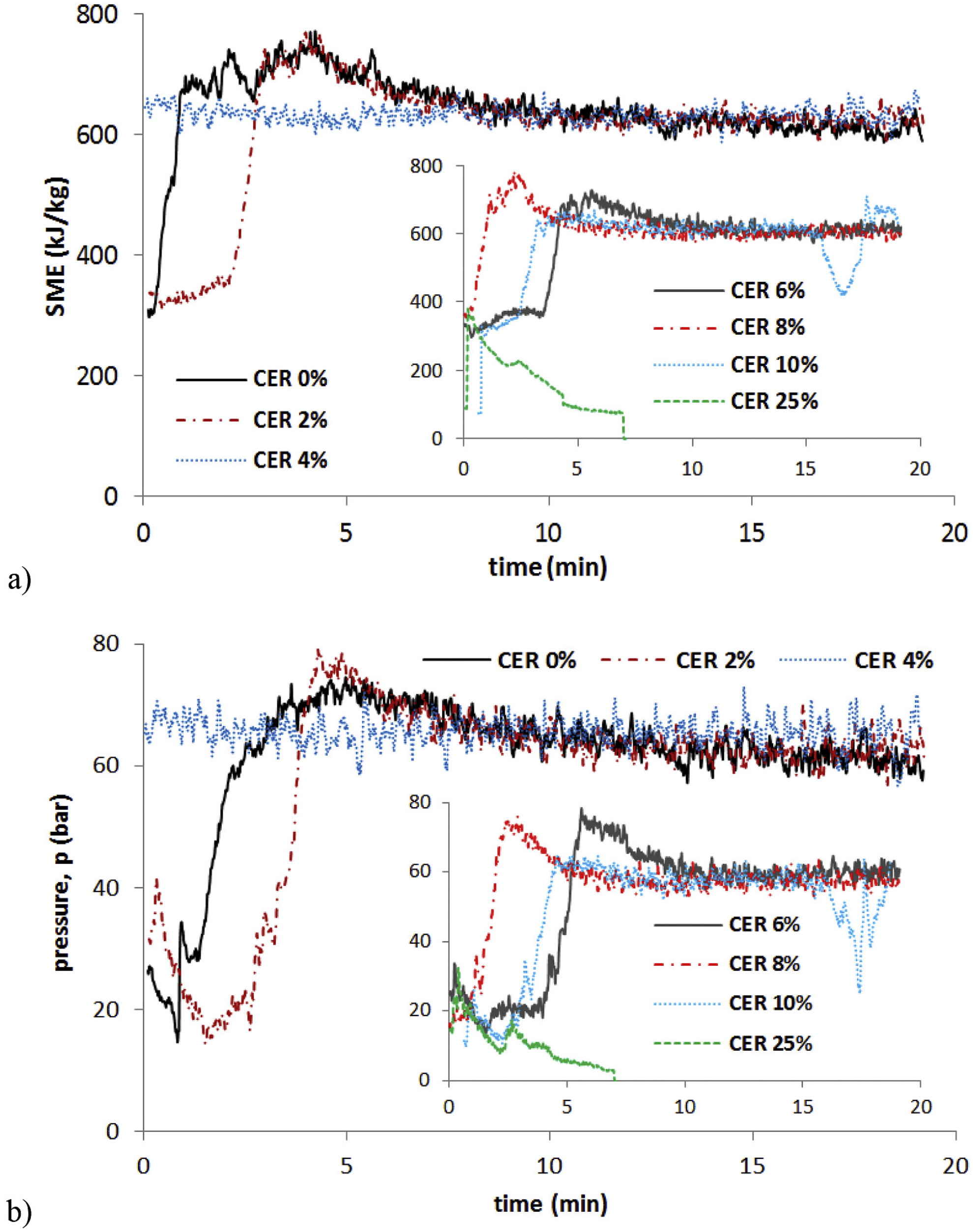

Fig. 2. Influence of moisture on SME (a) and extrusion pressures (b) during blending the IER with LDPE.

comparing the permselectivity for different counter-ions and IERs varying in water content, Geise et al. [42] found that permselectivity results cannot be explained only by water content. As the permselectivity begins to increase from 6% moisture, it is likely that the permselectivity changes are not caused by the initial content of moisture itself at the structural level but only at the macroscopic level. Therefore, the changes are induced by the properties of IER with artificially adjusted moisture, causing problems related to IER grinding and further processing steps during IEM manufacturing.

The main characteristic affecting permselectivity is the overall water uptake which IER can absorb (here about 50%, Table 1). No other IERs which differed in water swelling capacity were tested, so significant changes induced by structural reorganization due to how much water was absorbed could not be unambiguously confirmed. There are likely other issues connected to water content/permselectivity in which mechanisms have not been described in detail yet.

The mechanism of membrane selectivity can be related to a change in the parameters of diffusion movements of water molecules in various spatial scales of a membrane [43]. In certain conditions, clusters of water molecules can act as a space limiting factor in the ionic pathways of the membrane matrix [36]. These pathways can thus be controlled by ionic sites, so only counter-ions are able to pass through the membrane, thus increasing selectivity which is likely why the permselectivity begins to increase again from 6% moisture (Fig. 3).

In addition to Donnan repulsion, ions can be excluded from IER by dielectric effects. Dielectric exclusion refers to the tendency of ions to prefer partition into higher (water) and lower (water-swollen polymer) dielectric constant media [44]. For moistened IER introduced to a polymer matrix it follows that co-ions (Cl^- ions) were probably less soluble in swollen IER due to the lower dielectric

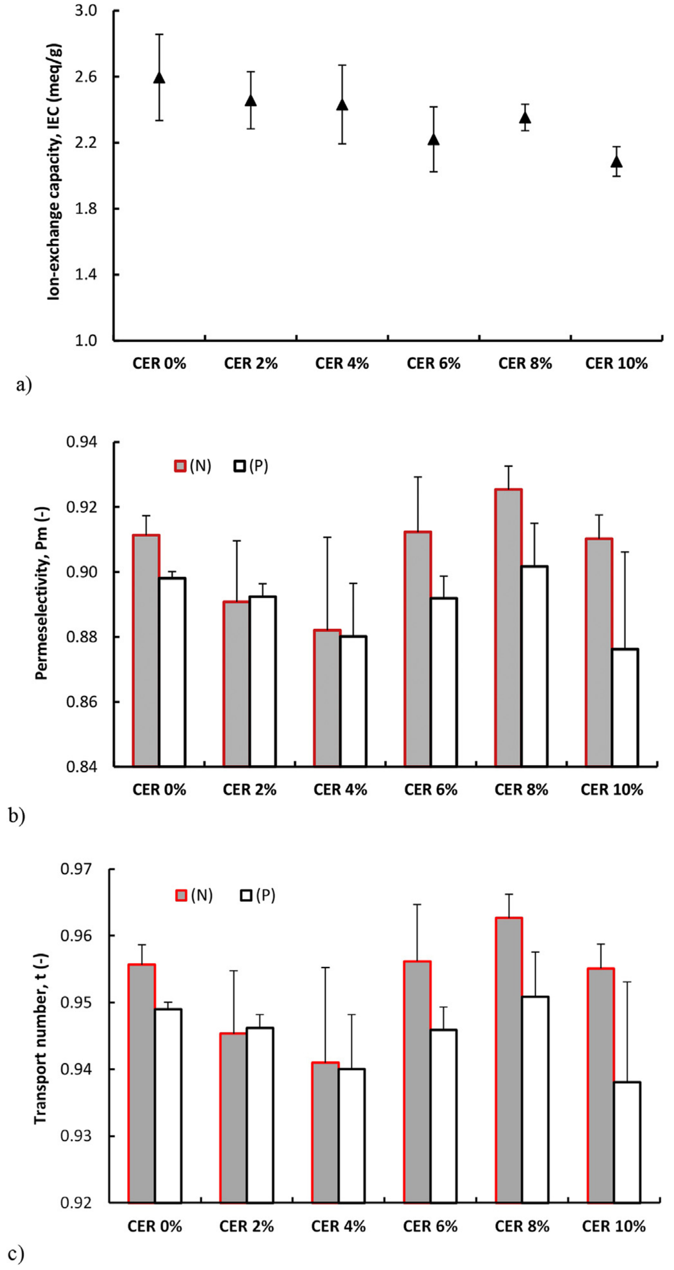

Fig. 3. Influence of CER moisture content on IEC (a), permselectivity (b) and transport number (c) of pressed (P) and non-pressed (N) membranes.

constant compared to water. This means that the higher dielectric exclusion of Cl^- ions out of the membrane could result in higher permselectivity in the range of moisture between 6 and 10%.

3.3.2. IEM electric resistance

Fig. 4 shows the change of resistance of (N) and (P) membranes with moisture. Specific and areal resistance increase with increasing moisture for both (N) and (P) membranes. For (P) membranes, the resistance is lower compared to (N). This is due mainly to a more uniform structure of the membrane after pressing. Generally, structural defects such as pores and other voids inevitably cause conductivity decrease. The overall membrane is more homogeneous and with less porosity due to pressing. In (N) membranes the influence of increasing moisture content is gradual. Both the specific and areal resistances of (N) membranes are two times higher than those of (P) membranes. Areal resistance of (P) increased by 61% from 2.98 to 4.88 Ω cm^2 in the moisture range of 0–8% (even though up to 6% it is almost constant) while for (N) it was by 52% from 6.15 to 11.89 Ω cm^2. The overall resistance increase with moisture is caused mainly by the inappropriate disintegration of IER particles with higher moisture, causing shifting particle size to higher values up to more than 100 μm (Fig. 1). The membrane structure is thus non-uniform with an increased number of inhomogeneities and pores causing conductivity loss. The areas of deteriorated conductivity are mainly IER/LDPE interfaces which change during IEM swelling/drying. The IER particles are introduced to the mixture in a partially swollen state, however, the subsequent extrusion and pressing causes water to evaporate, thus diminishing IER dimensions and causing higher porosity. This creates void spaces which are not involved in the ion exchange.

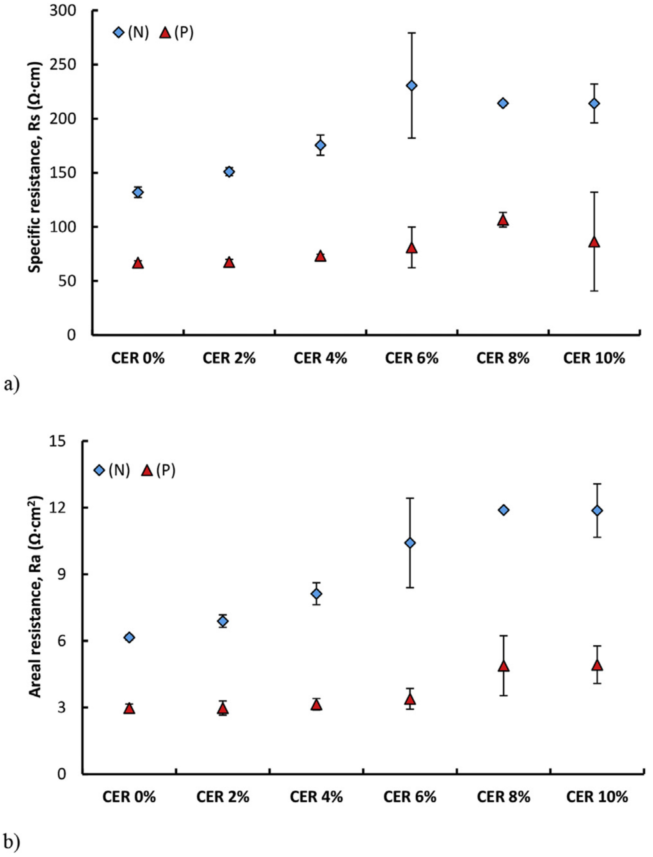

Fig. 4. Influence of CER moisture on specific (a) and areal (b) electric resistance of pressed (P) and non-pressed (N) IEMs.

Another question is how the initial moisture influences the membrane resistance at the micro-scale level of the IER particle itself, i.e. how the mechanism of ion transport is affected. So far, all the changes in electrochemical properties have been attributed to effects of moisture at the macroscale level, i.e. the detrimental effect of water-swollen IER particles in relation to IEM processing and the resulting properties. There are also potential reasons for resistance increase with IER moisture content at the level of a single IER particle.

It is generally known that dry IER particles are dielectrics (about 10^{-5} S/m) but with a sharp dependence of conductivity on moisture. This means that water or an electrolyte solution in contact with IER/IEM causes an abrupt increase in conductivity in a very narrow range of water content. This is related to the formation of ion and water transport channels in the IER/IEM microstructure, which is mostly influenced by external electric and concentration fields. The moisture (water molecules) is bonded in hydrate shells of fixed ion/counter ion pairs, immobilized in channels with effective radii in the range of 0.4–1.5 nm. The state of water is related to the hydrate capacity of the IER [19]. As the water molecules were introduced preliminarily (in the form of artificially adjusted moisture of IER), a part of the capacity was exhausted. This could contribute to the effects related to solution concentration on which the membrane conductivity is dependent [20,45].

Conductivity increases mostly in the concentration range of 0.5–1.5 M. For solutions exceeding 1.5 M, the conductivity decreases due mainly to Donnan's sorption of electrolyte and membrane dehydration. However, electrical resistances were determined using 0.5 M NaCl, which is the lower limit under the isoconductivity point in which the conductivity increases (i.e. resistance decreases) [19]. Nevertheless, the content of water molecules in the IER (mainly in the interstitial solution) contributes to dilution of the external NaCl solution [46]. Although the contribution of the water molecules is principally very small, in the limiting concentration region where abrupt concentration dependence of conductivity occurs, this can cause the resistance to increase. This resistance increase is higher with a higher amount of water molecules contributing to the external solution dilution, i.e. higher content of moisture. This hypothesis is, however, very limited since most of the moisture must have been evaporated during membrane preparation.

Adjusting the IER moisture content may be related to percolation (conductor-dielectric) transitions causing conductivity changes when varying the ratio between the conducting and non-conducting components. This was observed for several types of IEMs, such as poly(arylene sulfamides) in phenylone, poly(acrylic acid) in polypropylene and also PS-DVB in PE [47]. Conductivity decreases for the same reason as when IEC decreases due to the lower amount of dry IER. In IER with higher moisture, the lower amount of dry IER actively participating in the ion transport is per the same weight dosed during the blending of IER with LDPE. During preparation, and mainly for pressed membranes, the excess water is evaporated and the final weight of IER is lowest for IER with the highest moisture. The influence of pressing is clearly visible in Fig. 4, where pressed IEMs have lower resistances while increasing with higher initial IER moisture. The main reason for the resistance dependence shown in Fig. 4 is still the lower-quality processing and structure non-uniformity due to moist IER particles.

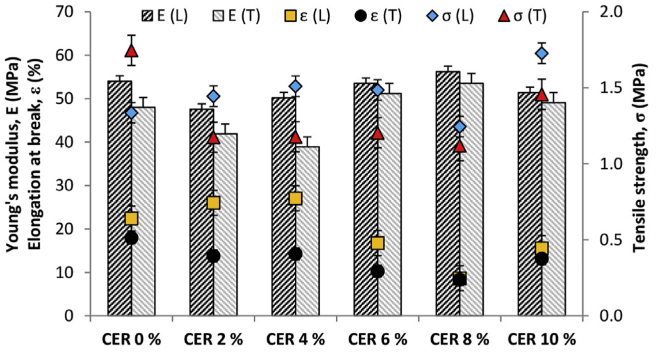

Fig. 5. Influence of moisture content of CER on mechanical properties of pressed IEMs in longitudinal (L) and transverse (T) direction.

3.4. *Effect of moisture on mechanical properties and microstructure*

Fig. 5 shows the mechanical properties of the IEM measured in the longitudinal (L) and transverse (T) directions. As the IEMs were not reinforced with a fabric these orthogonal directions were considered based on the extrusion process. During extrusion, the polymeric chains are oriented in the direction of extrusion which is the (L) direction while the perpendicular one is the (T) direction. Moreover, only pressed membranes were measured. Non-pressed membranes were not measured due to their non-uniform structure and problems with fixing in the testing machine, mainly their rupturing in clamping jaws.

Generally, mechanical properties in (L) are higher than in the (T) direction except for the stress of CER 0%. There is no definite trend in mechanical properties. The values are more or less constant and randomly varying, so the CER moisture has probably no significant effect on mechanical properties and variations are probably within the limits of experimental errors.

Fig. 6 shows the SEM images of the IEM's cross-sections with different moisture. We can see minimal change of the particle size and homogeneous distribution of particles in the matrix up to 4% of moisture. From the 6% moisture we can see flagrant change in microstructure characteristic of larger particles in the LDPE matrix and also worsened adhesion IER particles to LDPE matrix. However, this has minimal effect on the mechanical properties. The mechanical properties are mainly influenced by CER particle size and its content which is mostly about 60%. It was observed that with increasing IER loading, the membranes became more brittle, while the finer the IER, the more flexible IEM was obtained. It is possible to obtain flexible membranes up to an IER filling of 60% with a median particle size of 39 μm. The IEM becomes brittle with 40% of 80 μm IER particles [48]. The main reason for mechanical property variations is the change of IER grindability with moisture. Other issues related to mechanical properties may be the spatial distribution of IER particles and shape non-uniformity. Moreover, moisture in the IEM which was introduced during preparation due to moist IER may cause additional swelling, in turn causing other structural changes such as the significant displacement of IER particles and/or reinforcing fabric fibres from their original positions [49]. This is inevitably connected to mechanical property variations. A more in-depth study would have to be done in this area to obtain detailed results. Here, as no definite trend in the mechanical properties was obtained the main conclusion remains that it has a negligible effect.

4. Conclusions

This work aimed to determine the effect of IER moisture on the final properties of IEMs which has practical significance for industrial-scale devices utilizing IEMs. Based on the results presented above, the following conclusions were made:

- Increased IER moisture caused problems with grinding; the median particle size was shifted to higher values due to swelling and the formation of aggregates caused by enhanced adhesion forces. Moreover, swollen CER is less brittle (has higher toughness) so grinding is less efficient and its intensity is not very high with a constant grinding time.
- Aggregates formed at higher moisture can cause fluctuations in extruder response (most obvious for CER 10%) expressed by specific mechanical energy and extrusion head pressures due to unequal IER dosing.
- With an increase of IER initial moisture, the electrical resistances of IEMs gradually increased. This was mainly

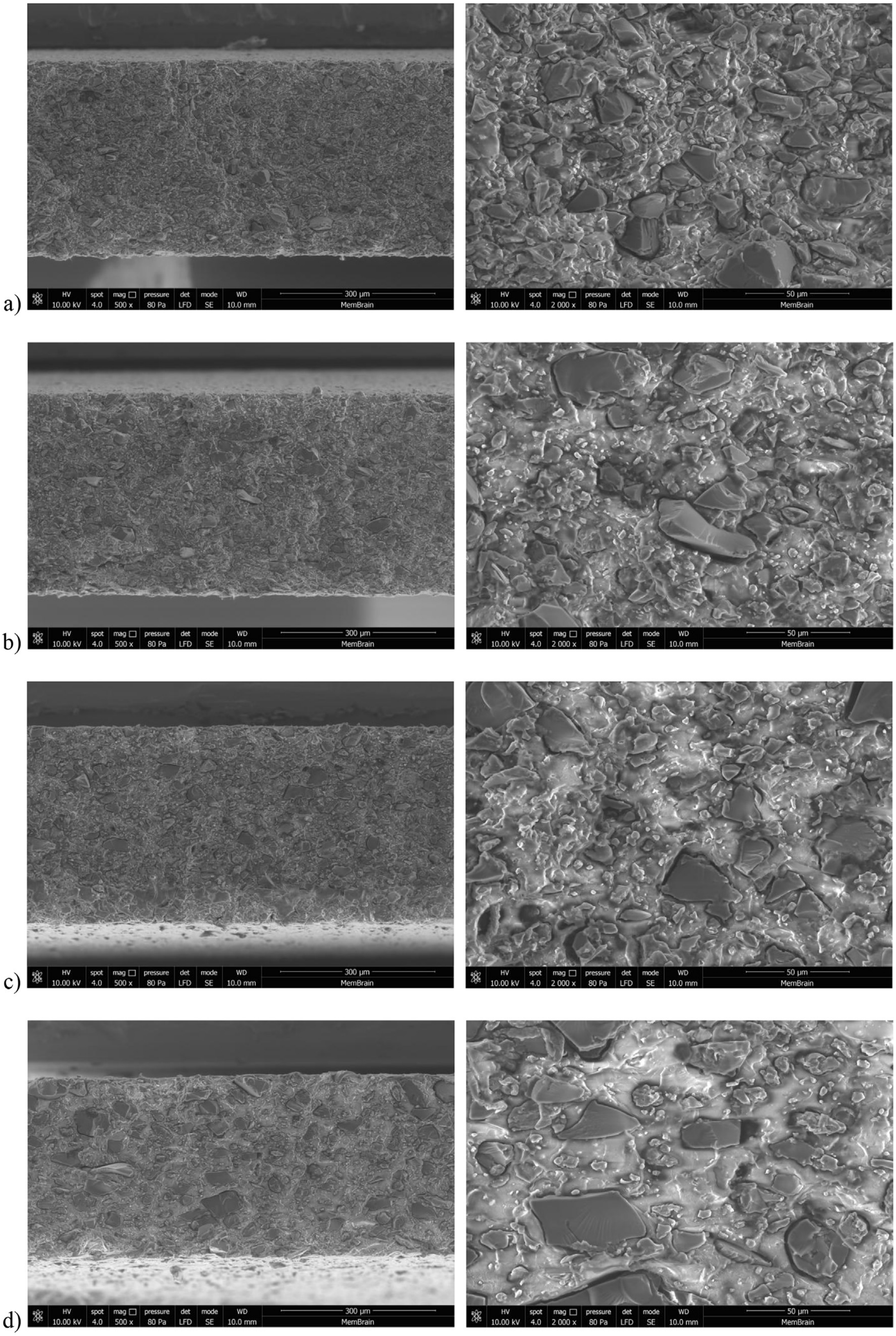

Fig. 6. Microstructure of IEMs' cross-section in overview (left) and in a detail (right): 0% (a), 2% (b), 4% (c), 6% (d), 8% (e) and 10% (f) moisture content.

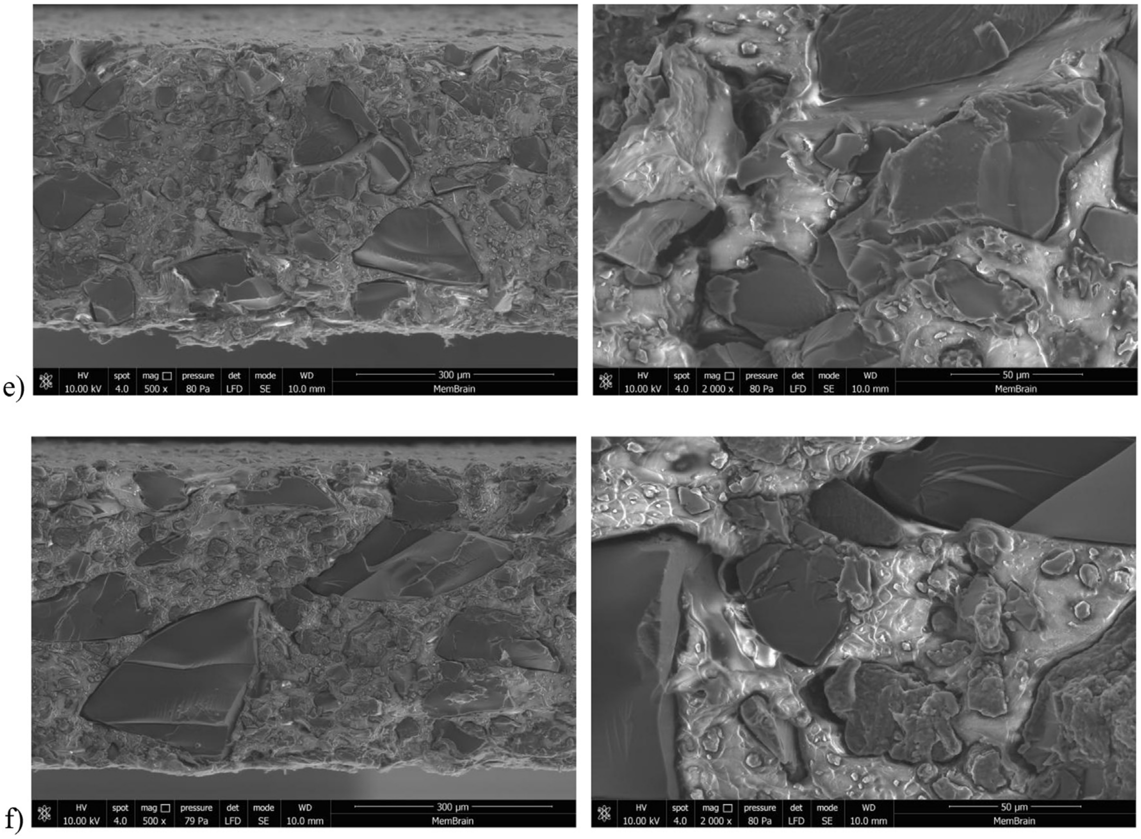

Fig. 6. (*continued*).

attributed to the less uniform structure of the final membranes, which was partially eliminated by IEM pressing.

- IEC decreases with increasing CER moisture content.
- Permselectivity and transport number did not show regular trends with increasing moisture. This was also true for mechanical properties.

Acknowledgement

The work was carried out within the framework of the project No. LO1418 “Progressive development of Membrane Innovation Centre” supported by the program NPU I Ministry of Education Youth and Sports of the Czech Republic, using the infrastructure Membrane Innovation Centre.

References

[1] E. Stránská, D. Neděla, R. Válek, J. Křivčík, Optimization of preparation of heterogeneous cation exchange membranes using different particle size distributions of ion exchange resins, Chem. Listy 109 (2015) 701–709 (In Czech).
[2] J. Křivčík, D. Neděla, R. Válek, Ion-exchange membrane reinforcing, Desalin. Water Treat. 56 (2015) 3214–3219.
[3] P. Bulejko, E. Stránská, K. Weinertová, Electrochemical and mechanical stability of ion-exchange membranes in alkaline solution, Chem. Pap. 71 (2017) 1303–1309.
[4] L. Alvarado, A. Chen, Electrodeionization: principles, strategies and applications, Electrochim. Acta 132 (2014) 583–597.
[5] H. Lu, Y. Wang, J. Wang, Recovery of Ni2 and pure water from electroplating rinse wastewater by an integrated two-stage electrodeionization process, J. Clean. Prod. 92 (2015) 257–266.
[6] S. Sun, Z. Shao, H. Yu, G. Li, B. Yi, Investigations on degradation of the long-term proton exchange membrane water electrolysis stack, J. Power Sources 267 (2014) 515–520.
[7] L. Zeng, T.S. Zhao, Integrated inorganic membrane electrode assembly with layered double hydroxides as ionic conductors for anion exchange membrane water electrolysis, Nano Energy 11 (2015) 110–118.
[8] M. Elangovan, S. Dharmalingam, Application of polysulphone based anion exchange membrane electrolyte for improved electricity generation in microbial fuel cell, Mater. Chem. Phys. 199 (2017) 528–536.
[9] S. Limpattayanate, M. Hunsom, Effect of supports on activity and stability of Pt–Pd catalysts for oxygen reduction reaction in proton exchange membrane fuel cells, J. Solid State Electrochem 17 (2013) 1221–1231.
[10] A. de Souza, E.R. Gonzalez, Influence of the operational parameters on the performance of polymer electrolyte membrane fuel cells with different flow fields, J. Solid State Electrochem 7 (2003) 651–657.
[11] D.-K. Kim, C. Duan, Y.-F. Chen, A. Majumdar, Power generation from concentration gradient by reverse electrodialysis in ion-selective nanochannels, Microfluid. Nanofluid 9 (2010) 1215–1224.
[12] J. Veerman, M. Saakes, S.J. Metz, G.J. Harmsen, Reverse electrodialysis: evaluation of suitable electrode systems, J. Appl. Electrochem 40 (2010) 1461–1474.
[13] K. Kwon, B.H. Park, D.H. Kim, D. Kim, Parametric study of reverse electrodialysis using ammonium bicarbonate solution for low-grade waste heat recovery, Energy Convers. Manage 103 (2015) 104–110.
[14] M. Tedesco, C. Scalici, D. Vaccari, A. Cipollina, A. Tamburini, G. Micale, Performance of the first reverse electrodialysis pilot plant for power production from saline waters and concentrated brines, J. Membr. Sci. 500 (2016) 33–45.
[15] J.G. Hong, B. Zhang, S. Glabman, N. Uzal, X. Dou, H. Zhang, et al., Potential ion exchange membranes and system performance in reverse electrodialysis for power generation: a review, J. Membr. Sci. 486 (2015) 71–88.
[16] E. Stránská, Relationships between transport and physical–mechanical properties of ion exchange membranes, Desalin. Water Treat. 56 (2015) 3220–3227.
[17] E. Lafond, C. Cau dit Coumes, S. Gauffinet, D. Chartier, L. Stefan, P. Le Bescop, Solidification of ion exchange resins saturated with Na ions: comparison of matrices based on Portland and blast furnace slag cement, J. Nucl. Mater 483 (2017) 121–131.
[18] A.B. Yaroslavtsev, V.V. Nikonenko, Ion-exchange membrane materials: properties, modification, and practical application, Nanotechnol. Russ. 4 (2009) 137–159.
[19] N.P. Berezina, N.A. Kononenko, O.A. Dyomina, N.P. Gnusin, Characterization of ion-exchange membrane materials: properties vs structure, Adv. Colloid Interface Sci. 139 (2008) 3–28.
[20] O.A. Dyomina, N.P. Berezina, A.V. Dyomin, V.I. Zabolotsky, Influence of aqueous–organic solutions containing aprotic solvent on equilibrium and transport properties of ion–exchange membranes, Desalination 240 (2009) 347–350.

[21] D.V. Golubenko, E.Y. Safronova, A.B. Ilyin, N.V. Shevlyakova, V.A. Tverskoi, L. Dammak, et al., Influence of the water state on the ionic conductivity of ion-exchange membranes based on polyethylene and sulfonated grafted polystyrene, Mater. Chem. Phys. 197 (2017) 192–199.

[22] J. Balster, M.H. Yildirim, D.F. Stamatialis, R. Ibanez, R.G.H. Lammertink, V. Jordan, M. Wessling, Morphology and microtopology of cation-exchange polymers and the origin of the overlimiting current, J. Phys. Chem. B 111 (2007) 2152–2165.

[23] N. Berezina, N. Gnusin, O. Dyomina, S. Timofeyev, Water electrotransport in membrane systems. Experiment and model description, J. Membr. Sci. 86 (1994) 207–229.

[24] D.C. Herbst, T.A. Witten, T.-H. Tsai, E.B. Coughlin, A.M. Maes, A.M. Herring, Water uptake profile in a model ion-exchange membrane: conditions for water-rich channels, J. Chem. Phys. 142 (2015), 114906–1-114906-21.

[25] M. Tedesco, H.V.M. Hamelers, P.M. Biesheuvel, Nernst-Planck transport theory for (reverse) electrodialysis: II. Effect of water transport through ion-exchange membranes, J. Membr. Sci. 531 (2017) 172–182.

[26] T. Yamanaka, T. Takeguchi, H. Takahashi, W. Ueda, Water transport during ion conduction in anion-exchange and cation-exchange membranes, J. Electrochem. Soc. 156 (2009) B831–B835.

[27] Y.S. Li, T.S. Zhao, W.W. Yang, Measurements of water uptake and transport properties in anion-exchange membranes, Int. J. Hydrogen Energ 35 (2010) 5656–5665.

[28] A. Roy, M.A. Hickner, H.-S. Lee, T. Glass, M. Paul, A. Badami, et al., States of water in proton exchange membranes: Part A - influence of chemical structure and composition, Polymer 111 (2017) 297–306.

[29] D. Neděla, J. Křivčík, R. Válek, E. Stránská, J. Marek, Influence of water content on properties of a heterogeneous bipolar membrane, Desalin. Water Treat. 56 (2015) 3269–3272.

[30] C. Jiang, Q. Wang, Y. Li, Y. Wang, T. Xu, Water electro-transport with hydrated cations in electrodialysis, Desalination 365 (2015) 204–212.

[31] A. Zlotorowicz, R.V. Strand, O.S. Burheim, Ø. Wilhelmsen, S. Kjelstrup, The permselectivity and water transference number of ion exchange membranes in reverse electrodialysis, J. Membr. Sci. 523 (2017) 402–408.

[32] Suqing Group Products, 2017. http://www.suqing.com/product_en.html. (Accessed 6 June 2017).

[33] Y. Fang, B. Zhang, Y. Wei, Effects of the specific mechanical energy on the physicochemical properties of texturized soy protein during high-moisture extrusion cooking, J. Food Eng. 121 (2014) 32–38.

[34] R. Osen, S. Toelstede, F. Wild, P. Eisner, U. Schweiggert-Weisz, High moisture extrusion cooking of pea protein isolates: raw material characteristics, extruder responses, and texture properties, J. Food Eng. 127 (2014) 67–74.

[35] X. Gao, A.I. Isayev, X. Zhang, J. Zhong, Influence of processing parameters during ultrasound assisted extrusion on the properties of polycarbonate/carbon nanotubes composites, Compos. Sci. Technol. 144 (2017) 125–138.

[36] T. Kikhavani, S.N. Ashrafizadeh, B. Van der Bruggen, Nitrate selectivity and transport properties of a novel anion exchange membrane in electrodialysis, Electrochim. Acta 144 (2014) 341–351.

[37] P. Bulejko, E. Stránská, K. Weinertová, Properties and structure of heterogeneous ion-exchange membranes after exposure to chemical agents, J. Solid State Electrochem 21 (2017) 111–124.

[38] J. Křivčík, D. Neděla, J. Hadrava, L. Brožová, Increasing selectivity of a heterogeneous ion-exchange membrane, Desalin. Water Treat. 56 (2015) 3160–3166.

[39] R. Takagi, M. Vaselbehagh, H. Matsuyama, Theoretical study of the permselectivity of an anion exchange membrane in electrodialysis, J. Membr. Sci. 470 (2014) 486–493.

[40] ČSN EN ISO 527–3, Plastics - Determination of Tensile Properties - Part 3: Test Conditions for Films and Sheets, 1997.

[41] A. Farahanchi, M.J. Sobkowicz, Kinetic and process modeling of thermal and mechanical degradation in ultrahigh speed twin screw extrusion, Polym. Degrad. Stab. 138 (2017) 40–46.

[42] G.M. Geise, H.J. Cassady, D.R. Paul, B.E. Logan, M.A. Hickner, Specific ion effects on membrane potential and the permselectivity of ion exchange membranes, Phys. Chem. Chem. Phys. 16 (2014) 21673–21681.

[43] V.V. Kotov, O.V. D'yakonova, S.A. Sokolova, V.I. Volkov, Structure and electrochemical properties of cation-exchange membranes based on partially imidized polyamidoacid, Russ. J. Electrochem 38 (2002) 888–891.

[44] A.E. Yaroshchuk, Dielectric exclusion of ions from membranes, Adv. Colloid Interface Sci. 85 (2000) 193–230.

[45] S.I. Niftaliev, O.A. Kozaderova, K.B. Kim, Electroconductance of heterogeneous ion-exchange membranes in aqueous salt solutions, J. Electroanal. Chem. 794 (2017) 58–63.

[46] X.T. Le, Permselectivity and microstructure of anion exchange membranes, J. Colloid Interf. Sci. 325 (2008) 215–222.

[47] N.P. Berezina, L.V. Karpenko, Percolation effects in ion-exchange materials, Colloid J. 62 (2000) 676–684.

[48] R.K. Nagarale, G.S. Gohil, V.K. Shahi, Recent developments on ion-exchange membranes and electro-membrane processes, Adv. Colloid Interface Sci. 119 (2006) 97–130.

[49] M. Svoboda, J. Beneš, L. Vobecká, Z. Slouka, Swelling induced structural changes of a heterogeneous cation-exchange membrane analyzed by micro-computed tomography, J. Membr. Sci. 525 (2017) 195–201.